Effect of Na/Ca Exchange on Plateau Fraction and $[Ca]_i$ in Models for Bursting in Pancreatic β-Cells

David Gall* and Isabella Susa#

*Laboratoire de Pharmacodynamie et Thérapeutique (CP617), Faculté de Médecine, Université Libre de Bruxelles, B-1070 Bruxelles, and #Unité de Chronobiologie Théorique (CP231), Faculté des Sciences, Université Libre de Bruxelles, B-1050 Bruxelles, Belgium

ABSTRACT In the presence of an insulinotropic glucose concentration, β-cells, in intact pancreatic islets, exhibit periodic bursting electrical activity consisting of an alternation of active and silent phases. The fraction of time spent in the active phase over a period is called the *plateau fraction* and is correlated with the rate of insulin release. However, the mechanisms that regulate the plateau fraction remain unclear. In this paper we investigate the possible role of the plasma membrane Na^+/Ca^{2+} exchange of the β-cell in controlling the plateau fraction. We have extended different single-cell models to incorporate this Ca^{2+}-activated electrogenic Ca^{2+} transporter. We find that the Na^+/Ca^{2+} exchange can provide a physiological mechanism to increase the plateau fraction as the glucose concentration is raised. In addition, we show theoretically that the Na^+/Ca^{2+} exchanger is a key regulator of the cytoplasmic calcium concentration in clusters of heterogeneous cells with gap-junctional electrical coupling.

INTRODUCTION

In physiological conditions, glycemia is tightly regulated. A major player involved in this control is insulin secreted by the pancreatic β-cells. Insulin is the only hormone preventing hyperglycemia. While secreting, pancreatic β-cells in intact islet of Langerhans exhibit periodic bursting electrical activity consisting of hyperpolarized silent phases alternating with depolarized active phases, during which fast action potentials occur (Dean and Matthews, 1970). It is well established that the elevation of the cytosolic free calcium concentration ($[Ca^{2+}]_i$) occurring during the active phase is involved in the triggering of exocytosis (Bokvist et al., 1995). Hence $[Ca^{2+}]_i$ regulation is of essential importance because of its role of second messenger in the stimulus-secretion coupling. Several transport mechanisms at the level of the plasma membrane are involved in this regulation, including L-type Ca^{2+} channels, Ca^{2+}-ATPases, and the Na^+/Ca^{2+} exchange. Since the first reports documenting the existence of a Na^+-dependent Ca^{2+} extrusion process in the heart (Reuter and Seitz, 1968) and the squid axon (Blaustein and Hodgkin, 1969), Na^+/Ca^{2+} exchange has been found in many other cell types, including pancreatic β-cells (Hellman et al., 1980; Herchuelz et al., 1980). Pancreatic islets, purified β-cells, and RINm5F cells all express several isoforms of the protein (Van Eylen et al., 1997). This antiporter uses the inward movement of the Na^+ ions down the Na^+ electrochemical gradient as an energy source for extruding Ca^{2+} from the cytosol. In cardiac myocyte, the Na^+/Ca^{2+} exchange plays a major role in returning the cells to basal $[Ca^{2+}]_i$ levels (Bers, 1991). Furthermore, because of the electrogenicity of the exchange reaction, the operation of the exchange gives rise to an inward current ($I_{Na/Ca}$), which is able to modulate the duration of the myocyte action potential (Egan et al., 1989; Noble et al., 1991). In the pancreatic β-cells, the physiological role of the Na^+/Ca^{2+} exchange remains unclear, but preliminary data indicate that it can regulate burst duration (Gall et al., 1999). The lack of specific inhibitors hinders the experimental assessment of the role of the Na^+/Ca^{2+} exchanger.

In this study, we have used mathematical modeling to explore the impact of the activity of this transporter, both on the $[Ca^{2+}]_i$ regulation and on the periodic bursting electrical activity. Of particular interest is the hypothesis that the Na^+/Ca^{2+} exchange is able to modulate the plateau fraction (Gall et al., 1999), i.e., the ratio of the duration of the active phase to the total bursting period, which is directly correlated with the amount of insulin secreted (Meissner and Schmelz, 1974). We have tested this hypothesis by including $I_{Na/Ca}$ in three single-cell models differing by the identity of the slow variable controlling the bursting electrical activity. In all of the proposed models, the presence of the exchanger leads to an increase in the plateau fraction. This shows that the modulation of the plateau fraction by the Na^+/Ca^{2+} exchange activity does not depend on a specific assumption concerning the precise mechanism underlying bursting. Furthermore, we examine a possible link between Na^+/Ca^{2+} exchange activity and glucose metabolism, which is provided by changes in the intracellular Na^+ concentration ($[Na^+]_i$). These single-cell models should be viewed as representing the behavior of a typical cell within a well-coupled islet.

Furthermore, we introduce a cluster model explicitly including electrical coupling between cells to study the effect of cell heterogeneity. As observed by Smolen et al. (1993), cellular heterogeneity induces high $[Ca^{2+}]_i$ values in some cells of the network. We have evaluated the role of the Na^+/Ca^{2+} exchange in the prevention of the occurrence of

Received for publication 16 November 1998 and in final form 5 April 1999.

Address reprint requests to Dr. Isabella Susa, Unité de Chronobiologie Théorique (CP231), Faculté des Sciences, Université Libre de Bruxelles, Boulevard du Triomphe, B-1050 Bruxelles, Belgium. Tel.: 32-2-650-54-41; Fax: 32-2-650-57-67; E-mail: isusa@ulb.ac.be.

0006-3495/99/07/45/09 $2.00

these local $[Ca^{2+}]_i$ peaks. Our simulations indicate that the Na^+/Ca^{2+} exchange is able to dramatically reduce local $[Ca^{2+}]_i$ peaks within the cluster.

ROLE OF THE Na^+/Ca^{2+} EXCHANGER IN SINGLE-CELL MODELS

The starting point of the mathematical models of membrane electrical activity of the pancreatic β-cell is the electrical circuit analogy. Following the classical approach of Hodgkin and Huxley (1952), the membrane can be considered as a leaky capacitor, and the membrane potential (V) dynamics are governed by the current balance equation:

$$C_m \frac{dV}{dt} = -\sum I_{ion} \quad (1)$$

where C_m is the total membrane capacitance and ΣI_{ion} is the sum of all ionic currents, depending on the type of channels considered in the model. The effect of the Na^+/Ca^{2+} exchange on the behavior of the β-cell electrical activity will be studied, including the current $I_{Na/Ca}$ in the current balance equation.

In cardiac myocytes and in most other tissues, the Na^+/Ca^{2+} exchanger appears to be a dominant transporter whenever large amounts of Ca^{2+} enter the cell. Measurements obtained in giant membrane patches (Hilgemann et al., 1992; Hilgemann, 1996) confirm that the Na^+/Ca^{2+} exchange is a high-capacity low-affinity transporter for Ca^{2+}. It appears that the exchanger protein is activated by $[Ca^{2+}]_i$ with a half-saturation constant, $K_{1/2}$, in the micromolar range. The single exchanger maximum turnover rate is on the order of 10^4 s^{-1}. Experimental I—V curves of Na^+/Ca^{2+} exchange in myocytes show a low conductance current in the range of $\sim$1 $\mu A/\mu F$ (Miura and Kimura, 1989), representing only a few percent of the steady-state membrane conductance. Furthermore, using the measurement of the reversal potential, several groups (Kimura et al., 1986; Ehara et al., 1989) were able to demonstrate unequivocally that the stoichiometry of the transmembranous exchange reaction is in agreement with the following scheme:

$$3Na_o + Ca_i \rightleftharpoons 3Na_i + Ca_o \quad (2)$$

where Na_o, Ca_o, Ca_i, and Na_i, respectively, are ions bound at the outer (o) and inner (i) binding sites of the transporter. The corresponding reversal potential is given by

$$V_{Na/Ca} = \frac{RT}{F}\left[3 \ln \frac{[Na^+]_o}{[Na^+]_i} - \ln \frac{[Ca^{2+}]_o}{[Ca^{2+}]_i}\right] \quad (3)$$

where R and F are the perfect gas and Faraday constants, T is the absolute temperature, $[Na^+]_o$ and $[Na^+]_i$ are the external and internal Na^+ concentrations, and $[Ca^{2+}]_o$ and $[Ca^{2+}]_i$ are the external and internal Ca^{2+} concentrations.

We base our model of $I_{Na/Ca}$ on the available data for the pancreatic β-cell (Gall et al., 1999), which are close to those found in myocytes. The I—V curves are almost linear, and the reversal potential follows Eq. 3. Hence we consider the exchanger as an ohmic conductor, and the corresponding current is

$$I_{Na/Ca} = g_{Na/Ca}(Ca_i)(V - V_{Na/Ca}) \quad (4)$$

with the whole-cell Na^+/Ca^{2+} conductance $g_{Na/Ca}(Ca_i)$ showing a sigmoidal dependence on $[Ca^{2+}]_i$:

$$g_{Na/Ca}(Ca_i) = \bar{g}_{Na/Ca} \frac{[Ca]_i^{n_H}}{K_{1/2}^{n_H} + [Ca]_i^{n_H}} \quad (5)$$

where $\bar{g}_{Na/Ca}$ is the maximum whole-cell Na^+/Ca^{2+} conductance, n_H is the Hill coefficient, and $K_{1/2}$ is the Ca^{2+} affinity constant of the exchanger. The parameter values and the precise expression of all of the ionic currents are listed in the Appendix. The equations of the single-cell models are numerically solved using a fourth-order Runge-Kutta method, as implemented in the subroutine D02BBF of the NAG library (Numerical Algorithms Group, Downers Grove, IL). Computations are performed on a SGI R10000 (Silicon Graphics, Mountain View, CA) workstation.

Model I

Our first model is the same as that of Gall et al. (1999) and is based on the model originally proposed by Sherman et al. (1988). In this model, $[Ca^{2+}]_i$ plays the role of the slow variable causing the switch between the active and the silent phase through the activation of the K(Ca) channels. This hypothesis, first proposed by Atwater et al. (1980), was abandoned when it was shown (Kukuljan et al., 1991) that charybdotoxin (ChTX), a blocker of the large-conductance K(Ca) channels, failed to affect the bursting pattern. However, recent data (Göpel and Rorsman, 1998) indicate the existence of a ChTX-insensitive K(Ca) current that may be involved in the termination of the burst.

The fast subsystem describing the action potential dynamics is given by

$$C_m \frac{dV}{dt} = -I_K - I_{Ca} - I_{K(Ca)} - I_{Na/Ca} \quad (6)$$

$$\frac{dn}{dt} = \lambda \frac{n_\infty(V) - n}{\tau_n(V)} \quad (7)$$

where I_K is the delayed rectifier K^+ current, I_{Ca} is the voltage-dependent L-type Ca^{2+} current, $I_{K(Ca)}$ is the Ca^{2+}-activated K^+ current, and n is the gating variable for the delayed-rectifier K^+ channel. Because $I_{Na/Ca}$ is produced by a Ca^{2+} transporter, it must also appear in the $[Ca^{2+}]_i$ balance equation:

$$\frac{dCa_i}{dt} = f[-\alpha(I_{Ca} - 2I_{Na/Ca}) - k_{Ca}Ca_i] \quad (8)$$

The precise expression of all of the currents and the parameter values are given in the Appendix. Equations 6, 7, and 8 constitute model I. Fig. 1, *a* and *b*, shows the voltage and

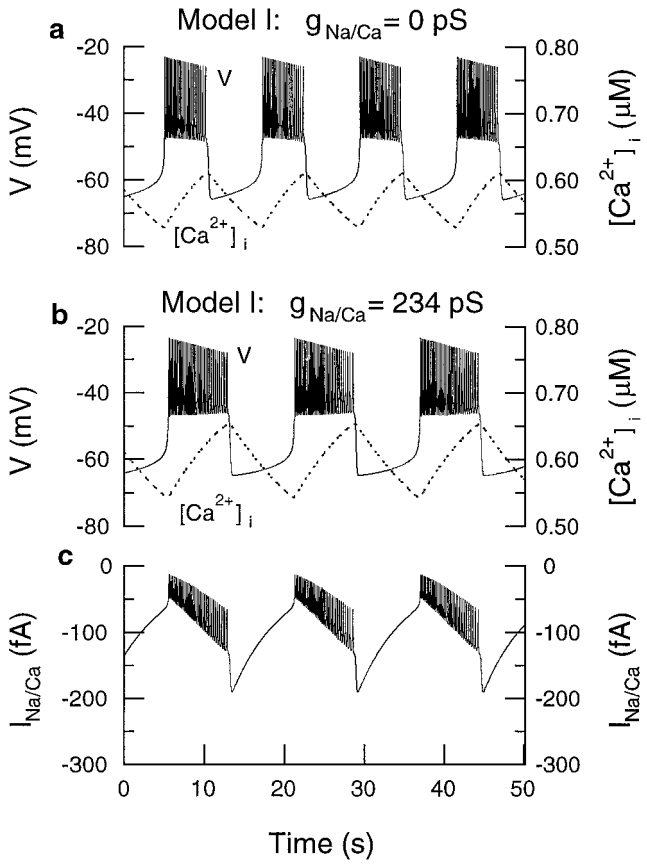

FIGURE 1 Membrane potential, V (——), and free intracellular calcium, $[Ca^{2+}]_i$, (- - - -) for model I, in the absence (*a*) and in the presence (*b*) of Na^+/Ca^{2+} exchange activity; the curves are obtained by numerical integration of Eqs. 6, 7, and 8. Parameter values are listed in the Appendix. Using the same parameters values as in *b*, the Na^+/Ca^{2+} exchange current, $I_{Na/Ca}$, is shown in *c*. Note the plateau fraction increase from 0.41 to 0.46 when the Na^+/Ca^{2+} exchange is present.

cytosolic free Ca^{2+} concentration time courses, obtained by numerical integration of the equations of model I, in the absence ($\bar{g}_{Na/Ca}$ = 0 pS) and in the presence ($\bar{g}_{Na/Ca}$ = 234 pS) of Na^+/Ca^{2+} exchange activity. These pictures show that the exchanger is able to prolong the burst duration. It should be noted that this prolongation of the active phase is not due to a change in calcium dynamics that would postpone the activation of the Ca^{2+}-activated K^+ current. In fact, $[Ca^{2+}]_i$ is even higher in the presence of the Na^+/Ca^{2+} exchange than in its absence. It is thus solely the depolarizing influence of $I_{Na/Ca}$ that prolongs the burst. Fig. 1 *c* shows the time course of $I_{Na/Ca}$, which reaches its peak value at the end of each burst. Note that the exchanger does not reverse during the electrical activity and thus never provides an additional Ca^{2+} entry mechanism to the cell.

Model II

The spectrophotometric measurements of Santos et al. (1991) show that the time scale of $[Ca^{2+}]_i$ change is short relative to the burst period. In these experiments, a rapid increase in $[Ca^{2+}]_i$ accompanies the beginning of the active phase and, during the silent phase, $[Ca^{2+}]_i$ decreases slowly. However, model I predicts sawtooth-shaped oscillations in $[Ca^{2+}]_i$ instead of the square waves that have been measured. To take into account these experimental facts, we have to consider a model in which $[Ca^{2+}]_i$ is a fast variable. As the identity of the physiological slow variable that drives bursting remains unclear, Sherman (1996) has proposed a general model in which $[Ca^{2+}]_i$ is fast. In this model, an ad hoc slow variable s activates a hyperpolarizing current, I_{slow}, allowing the switch between the active and silent phases. We will use the same approach to study the effect of Na^+/Ca^{2+} exchange activity in a model in which $[Ca^{2+}]_i$ is a fast variable.

The equations describing the dynamics of V and the gating variables n and s in model II are given by

$$C_m \frac{dV}{dt} = -I_K - I_{Ca} - I_{slow} - I_{Na/Ca} \tag{9}$$

$$\frac{dn}{dt} = \frac{n_\infty(V) - n}{\tau_n} \tag{10}$$

$$\frac{ds}{dt} = \frac{S(V, R_s) - s}{\tau_s} \tag{11}$$

We have also incorporated Ca^{2+} transport between the cytosol and the endoplasmic reticulum (ER). As in a previous study (Chay, 1997), we do not consider the calcium-induced calcium release mechanism for the calcium release from the ER. During the bursts, when the L-type Ca^{2+} channels are open, the Ca^{2+} is pumped from the cytosol in the ER. This Ca^{2+} accumulated in the ER is then gradually released in the cytosol during the silent phase. This allows a gradual rather than steep decrease in $[Ca^{2+}]_i$ during the silent phase, as observed by Santos et al. (1991). Thus Eq. 8 becomes

$$\frac{d[Ca]_i}{dt} = f[-\alpha(I_{Ca} - 2I_{Na/Ca}) - k_{Ca}[Ca]_i] + k_{rel}([Ca]_{ret} - [Ca]_i) - k_{pump}[Ca]_i \tag{12}$$

where f is the fraction of free cytoplasmic Ca^{2+}, and α is a factor that converts current into concentration changes. Parameter k_{Ca} is the Ca^{2+} removal rate by mechanisms other than sequestration in the ER. The last two terms in Eq. 12 are due to the presence of the ER, the evolution of the calcium concentration in the ER ($[Ca^{2+}]_{ret}$) being given by

$$\frac{d[Ca]_{ret}}{dt} = -k_{rel}([Ca]_{ret} - [Ca]_i) + k_{pump}[Ca]_i \tag{13}$$

where k_{rel} reflects the calcium release of the ER and k_{pump} is the pump activity of the Ca^{2+}-ATPase in the ER, which is taken here as linear. As observed by Bokvist et al. (1995), the entry of Ca^{2+} in the pancreatic β-cell is concentrated in a "hot spot," where the L-type Ca^{2+} channels and the secretory granules are colocalized. It should be noted that

$[Ca^{2+}]_i$ in this model corresponds to the Ca^{2+} concentration in this compartment. For the sake of simplicity, we consider the cytosolic compartment and the ER to have identical volumes and buffering capacities.

Model II is constituted by Eqs. 9–13 (details concerning the expressions for the various currents and the parameters are given in the Appendix). The bursting in model II is shown in Fig. 2. The curves in Fig. 2, *a* and *b*, were obtained by solving numerically the differential equations in model II, in the absence and in the presence of Na^+/Ca^{2+} exchange activity. The slow rise and fall of the slow variable *s* (*dotted line*), which activates I_{slow}, drives the membrane potential (*solid line*) oscillations. Fig. 2 *c* shows the corresponding levels of $[Ca^{2+}]_i$ (*solid line*) and $[Ca^{2+}]_{ret}$ (*dotted line*). Note that $[Ca^{2+}]_i$ here is a fast variable, in contrast to the case illustrated in Fig. 1. As in model I, the presence of the Na^+/Ca^{2+} exchange induces a substantial prolongation of the active phase.

Model III

We have seen in the previous section that model II provides a general model for bursting. However, the slow variable *s* lacks physiological grounding. Furthermore, this model includes two slow variables, $[Ca^{2+}]_{ret}$ and *s*, where only one is needed to produce bursting. Chay (1997) has proposed several models in which the dynamics of Ca^{2+} in the ER is the only slow variable driving the electrical bursting. A way to include this hypothesis is to replace the three equations 9–11 from model II with Eqs. 6 and 7. Consequently, the bursting now relies on a Ca^{2+}-activated K^+ current rather than on I_{slow}. The $[Ca^{2+}]_i$ and $[Ca^{2+}]_{ret}$ dynamics are included in the model via Eqs. 12 and 13. These four equations define model III.

The slow oscillation of Ca^{2+} in the ER in model III is shown in Fig. 3 *b* (*dotted line*) along with the membrane potential (*solid line*). In Fig. 3 *c*, the corresponding $[Ca^{2+}]_i$ is represented by a solid curve. Fig. 3, *a* and *b*, shows the electrical activity, in the absence and in the presence of Na^+/Ca^{2+} exchange activity. Once again, the presence of

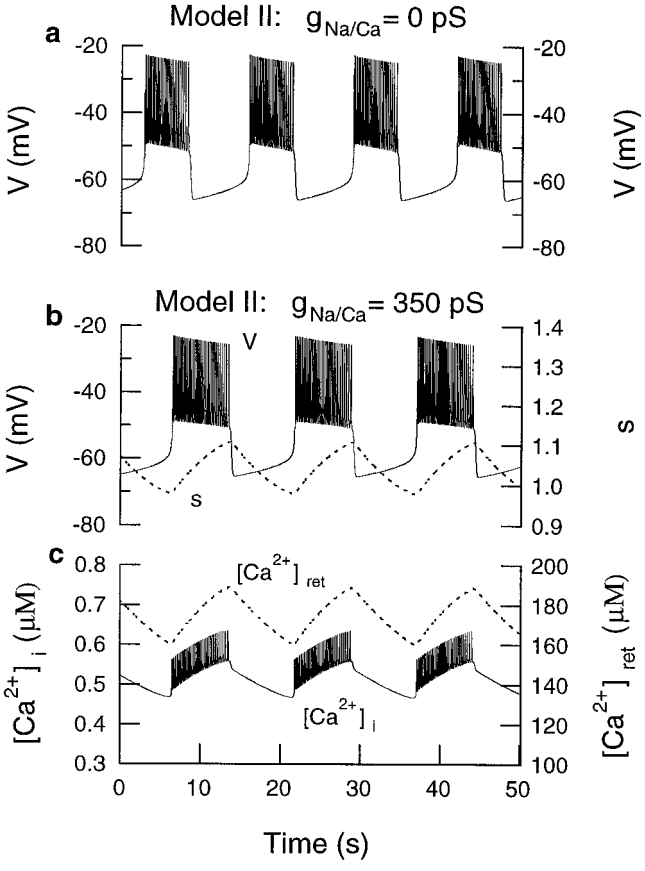

FIGURE 2 Bursting in model II in the absence (*a*) and in the presence (*b*) of Na^+/Ca^{2+} exchange activity. Shown are voltage, *V* (——), and the slow gating variable, *s* (- - - -), of the hyperpolarizing current, I_{slow}. Using the same parameters as in *b*, *c* shows the intracellular calcium concentration, $[Ca^{2+}]_i$, and the slow variation of calcium in the endoplasmic reticulum, $[Ca^{2+}]_{ret}$ (- - - -). The curves were obtained by integrating numerically 9, 10, 11, 12, and 13 for the parameter values listed in the Appendix. There is an increase in the plateau fraction from 0.41 to 0.45 when the Na^+/Ca^{2+} exchange is present.

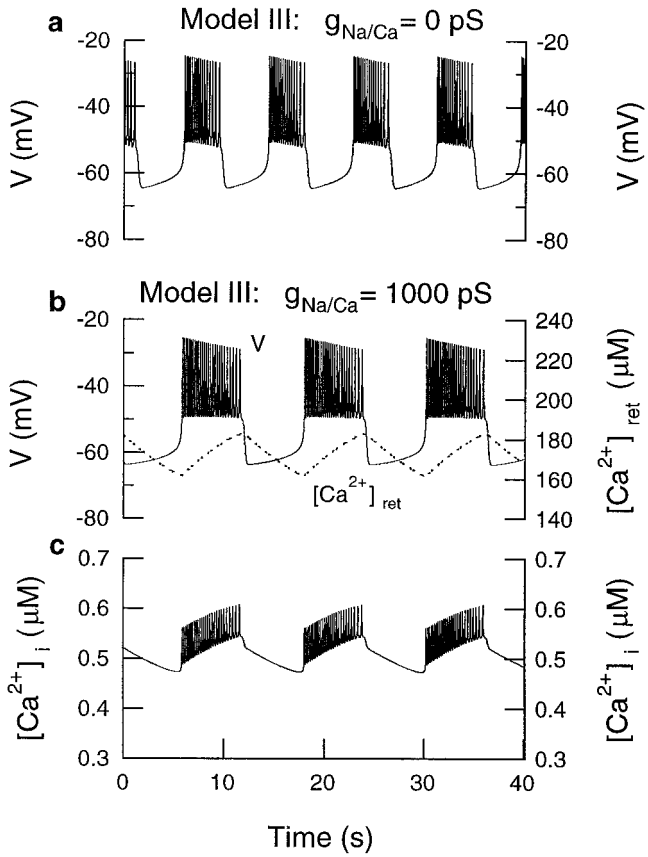

FIGURE 3 Bursting in model III. Computed solutions of Eqs. 6, 7, 12, and 13 in the absence (*a*) and in the presence (*b*) of Na^+/Ca^{2+} exchange activity: time courses of electrical activity, *V* (——), and of the endoplasmic reticulum calcium concentration, $[Ca^{2+}]_{ret}$ (- - - -), which regulates bursting in model III. Plateau fraction increases from 0.41 to 0.47 when Na^+/Ca^{2+} exchange is present. Using the same parameters as in *b*, *c* shows the oscillation of the intracellular calcium concentration, $[Ca^{2+}]_i$ (see the Appendix for parameter values).

the Na^+/Ca^{2+} exchange induces an increase in the duration of the bursts.

Influence of the Na^+/Ca^{2+} exchange on the plateau fraction

To examine the physiological relevance of this prolongation of the active phase, we evaluate the plateau fraction in the absence and in the presence of the transporter. The plateau fraction is defined as the ratio of the active phase duration to the burst period. The active phase is measured as the time separating the local membrane potential maxima of the first and last spikes during a burst. In the numerical simulation of Fig. 1, the presence of the Na^+/Ca^{2+} exchange activity corresponds to an increase in the plateau fraction from 0.41 to 0.46. This finding demonstrates the ability of the Na^+/Ca^{2+} exchange to modulate the plateau fraction and thus, possibly, the insulin secretion. Let us recall that it is not possible, so far, to assess experimentally the contribution of the Na^+/Ca^{2+} exchange to the stimulus-secretion coupling, in view of the lack of specific inhibitor.

To check that the modulation of the plateau fraction by the Na^+/Ca^{2+} exchange is a model-independent feature, we now turn to models II and III. For ease of comparison, in all three models, the parameters are carefully chosen to obtain a similar value of the plateau fraction in the absence of Na^+/Ca^{2+} exchange activity, and $g_{Na/Ca}$ is properly scaled to ensure that $I_{Na/Ca}$ is of similar relative intensity (~5% of the total membrane current). Figs. 2, *a* and *b*, and 3, *a* and *b*, are obtained, integrating numerically the differential equations in models II and III, in the absence and in the presence of Na^+/Ca^{2+} exchange activity. As in model I, the presence of the Na^+/Ca^{2+} exchange induces an increase in the plateau fraction, from 0.41 to 0.45 in model II and from 0.41 to 0.47 in model III.

Thus, despite the differences in the bursting mechanism, the changes in plateau fraction due to the contribution of the Na^+/Ca^{2+} exchange are qualitatively similar in the three models.

Glucose sensitivity of $I_{Na/Ca}$

In a physiological context, the ability of the Na^+/Ca^{2+} exchange to modulate the plateau fraction only makes sense if there is a relationship between the activity of the transporter and extracellular glucose concentration. This would allow the Na^+/Ca^{2+} exchange to contribute to the progressive increase of the plateau fraction, from 0 to 1, which is observed when the extracellular glucose concentration is raised.

It is known that an increase in extracellular glucose decreases the Na^+ content in pancreatic islets (Wesslen et al., 1986). Using spectrophotometric measurements in clusters of islet cells, Saha and Grapengiesser (1995) observe a decrease in the steady-state $[Na^+]_i$ from 14 mM to 11 mM when the extracellular glucose concentration is raised from 3 mM to 20 mM. On the other hand, a reduction in $[Na^+]_i$ shifts the reversal potential of the Na^+/Ca^{2+} exchange toward more positive voltage, increasing the driving force on the exchanger and thus $I_{Na/Ca}$. Therefore $[Na^+]_i$ could provide the link between extracellular glucose and increased Na^+/Ca^{2+} exchange activity.

In Fig. 4, we explore the ability of the Na^+/Ca^{2+} exchange current to increase the plateau fraction as $[Na^+]_i$ is decreased. A lowering of $[Na^+]_i$ from 15 mM to 9 mM results in an 11% increase of the plateau fraction in model III. The corresponding plateau fraction increase is more modest in model I (7%) and model II (3%). The jaggedness in the plateau fraction curves simply reflects the discontinuous variation of the active phase duration, which is measured as the time separating the local membrane potential maxima of the first and last spikes during a burst. As the bursts become longer when $[Na^+]_i$ is decreased, the number of spikes per burst increases. Each time a new spike is added to the burst, the active phase duration increases in a discontinuous manner.

ROLE OF THE Na^+/Ca^{2+} EXCHANGER IN A HETEROGENEOUS CLUSTER MODEL

Cluster model for β-cells coupled through gap junctions

The β-cells are grouped in pancreatic islets. Their number within an islet is estimated to be on the order of 3000–4000

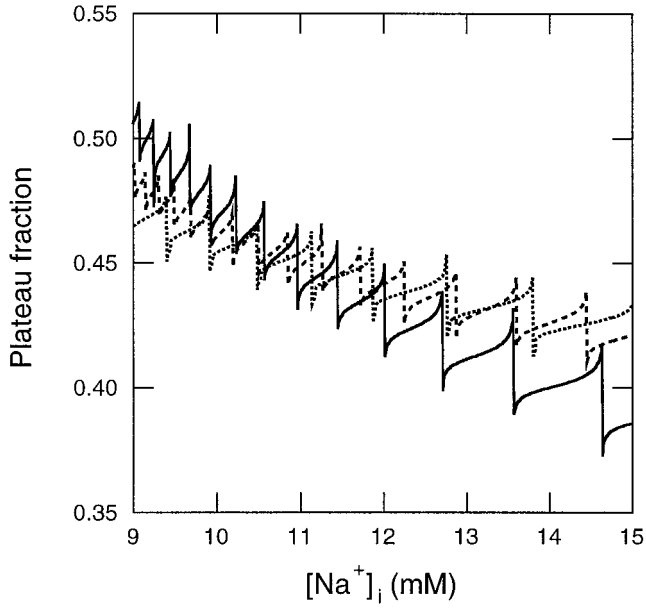

FIGURE 4 Effect of $[Na^+]_i$ on the plateau fraction. The plateau fraction is shown as a function of the intracellular Na^+ concentration in model I (- - -), model II (·····), and model III (——). The jaggedness of the plateau fraction curves is due to the necessarily discrete variation of the number of spikes per burst when $[Na^+]_i$ is decreased. This induces discontinuities in the active phase duration whenever there is a transition from n to $n + 1$ spikes per burst.

in the pancreas of an adult mouse. They constitute more than 50% of each islet and are interconnected by gap junctions (Meissner, 1976). Gap junctions are dynamic structures allowing the passage of ions and other small molecules and, probably, the subsequent synchronization of adjacent β-cells.

Models such as the ones introduced above describe the electrical behavior of a typical cell within a well-coupled islet. In this section, we explicitly introduce a cluster model including electrical coupling between cells to study the effect of cell heterogeneity on $[Ca^{2+}]_i$ dynamics. Like Smolen et al. (1993), we consider a cellular network corresponding to the gap-junctional coupling of heterogeneous cells that differ in size, channel properties, and other parameters. Smolen et al. (1993) show that for a sufficiently large cluster ($\sim$125 cells) of such cells, the bursting is synchronous. However, with the chosen distribution of parameters, only a few cells would burst if they were uncoupled.

Our theoretical study of the coupled cell system has been realized considering, in turn, that the behavior of each single cell is described by model I, II, or III (see previous section). We show the results only for model III, but there is no qualitative difference with the other cases. The equations of the model for a cluster of $N = n \times n$ cells are given by

$$C_m \frac{dV_j}{dt} = -I_{K,j} - I_{Ca,j} - I_{K(Ca),j} - I_{Na/Ca,j} - \sum_k g_{j,k}(V_j - V_k)$$

$$j = 1 \ldots N \quad (14)$$

where the summation is over the four first neighbors k of cell j. The expression of the different currents is the same as that given in the Appendix for model III, with variables and distributed parameters indexed by cell number. We use the gap-junction conductance values determined experimentally (Perez-Armendariz et al., 1985). Gap-junctional coupling only affects the V_j variables, so that the differential equations for n, Ca^{2+}, and $[Ca^{2+}]_{ret}$ are the same as Eqs. 7, 12, and 13 for model III, indexed by cell number.

The complete system is composed of $4N$ differential equations (14) and the equations for n_j, $[Ca^{2+}]_{i_j}$, $[Ca^{2+}]_{ret_j}$ ($j = 1 \ldots N$). The boundary conditions have been chosen to be periodic.

The parameters listed in the Appendix are lognormally distributed with a 15% standard deviation. For the distributed parameters, we chose an average value equal to the one used in the simulation of the single-cell model III. The average numerical value of the maximum Na^+/Ca^{2+} exchange conductance ($\langle \bar{g}_{Na/Ca} \rangle = 550$ pS) has been chosen to obtain, in the cluster model, $I_{Na/Ca}$ of a relative intensity similar to that in the single-cell models. The numerical simulations have been performed with a homemade routine based on a second-order predictor-corrector method (Heun's method). In all of the numerical experiments presented below, we have chosen $n = 15$, which corresponds to 225 cells.

Fig. 5 shows the bursting of a typical cell of the 15×15 network of cells. The bursts in the network are synchronous because of the gap-junctional coupling between cells.

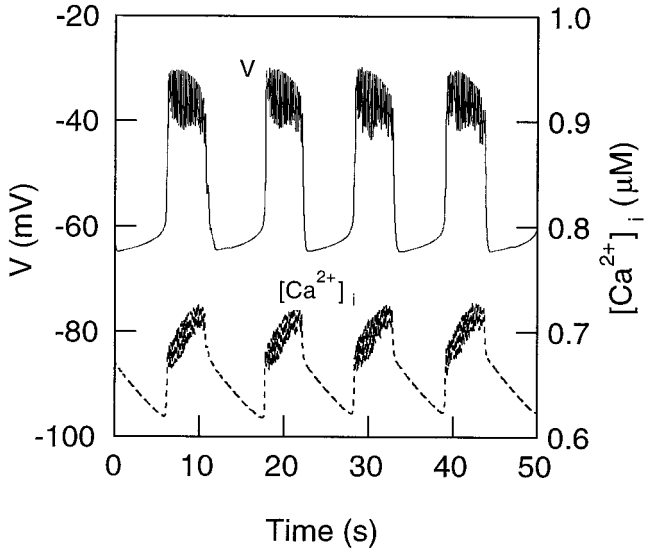

FIGURE 5 Cellular bursting dynamics in the cluster model. Shown are the evolution of V (——) and $[Ca^{2+}]_i$ (- - -) during the bursting electrical activity of a typical cell inside a 15×15 network of cells coupled by gap junctions in the presence of Na^+/Ca^{2+} exchange activity. Some parameter values are distributed over the network in a heterogeneous manner (see the text).

Calcium dynamics in the cluster model

In Fig. 6 we compare the calcium levels in the presence (*solid curves*) or absence (*dashed curves*) of the Na^+/Ca^{2+} exchange for one cell of the network (Fig. 6 *a*) and for the average over all of the cells of the cluster (Fig. 6 *b*).

Because of the heterogeneity of cell parameter values in the numerical simulations, $[Ca^{2+}]_i$ can attain high levels ($\sim$1 μM) in some cells. To prevent this situation, Smolen et al. (1993) had to postulate an additional mechanism of calcium uptake from the cytosol, strongly activating at high $[Ca^{2+}]_i$ levels.

Fig. 6 *a* shows the time evolution of the $[Ca^{2+}]_i$ of a cell producing a calcium peak ($\simeq$0.95 μM) when the Na^+/Ca^{2+} exchanger is absent (*solid line*). The same cell displays a lower $[Ca^{2+}]_i$ level when the Na^+/Ca^{2+} exchange is active, with an average value of the conductance $g_{Na/Ca}$ of 550 pS (*dashed line*). This means that, locally, the Na^+/Ca^{2+} exchange can be a major mechanism of Ca^{2+} extrusion, preventing high $[Ca^{2+}]_i$ peaks.

As previously observed, the depolarizing effect of the $I_{Na/Ca}$ current prolongs the burst and consequently increases the $[Ca^{2+}]_i$ entering through the L-type calcium channels. This is still true in the multicellular model, except for the cells in which $[Ca^{2+}]_i$ reaches unphysiologically high levels. Fig. 6 *b* presents the temporal variation of the cytosolic free Ca^{2+} concentration averaged over all cells of the network. This $[Ca^{2+}]_i$ averaged value is higher when the $Na^+/$

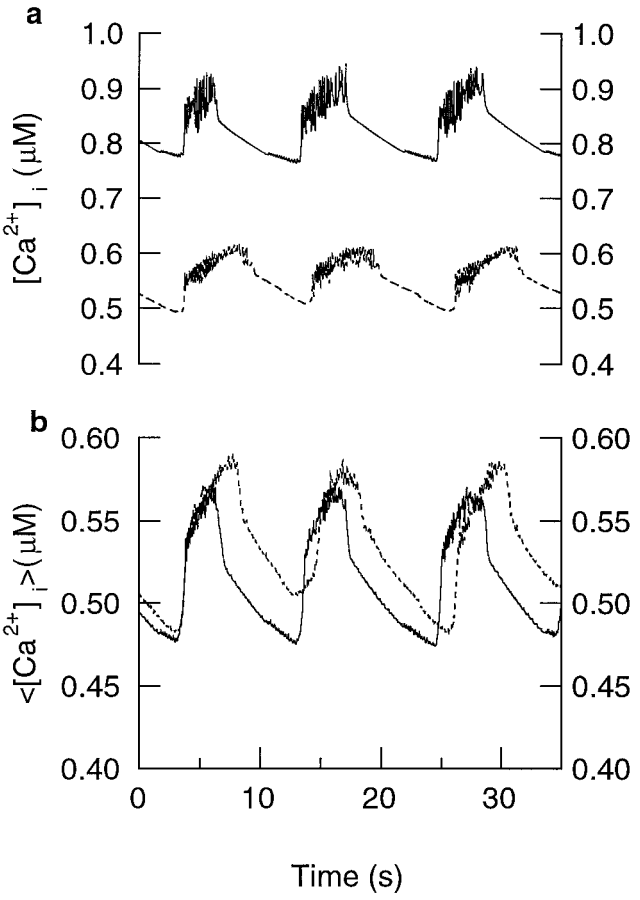

FIGURE 6 Calcium dynamics in a cluster of coupled heterogeneous β-cells. Shown is the $[Ca^{2+}]_i$ of a cell of the 15 × 15 network displaying a $[Ca^{2+}]_i$ peak in the absence of Na^+/Ca^{2+} exchange activity (*a*, ——). The $[Ca^{2+}]_i$ value for the same cell is dramatically decreased in the presence ($\bar{g}_{Na/Ca}$ = 584.6 pS) of the Na^+/Ca^{2+} activity (*a*, - - -). The value of the Na/Ca exchange maximum conductance is attributed by the lognormal distribution with average 550 pS and 15% standard deviation. For the same numerical simulations, *b* shows the $[Ca^{2+}]_i$ averaged over all of the cells of the network, when the Na^+/Ca^{2+} exchange is inactivated (——) and active (- - -). Note the increase in the averaged $[Ca^{2+}]_i$ when the Na^+/Ca^{2+} exchange is present.

Ca^{2+} exchange is active (*dashed curve*) than when $g_{Na/Ca}$ = 0 (*solid line*).

The same qualitative results have been obtained when networks of cells described by models I and II were considered. The reduction of calcium peaks by the Na^+/Ca^{2+} exchanger is therefore a model-independent feature.

DISCUSSION

We have used mathematical models to investigate the role of Na^+/Ca^{2+} exchange in the bursting activity of pancreatic β-cells. Our starting point was a modification of the model proposed by Sherman et al. (1988). This modification (model I) takes into account the contribution of the Na^+/Ca^{2+} exchange current to the dynamics of voltage and $[Ca^{2+}]_i$ (Gall et al., 1999). Our simulations with model I indicate that the presence of Na^+/Ca^{2+} exchange activity can substantially increase the plateau fraction of the bursting electrical activity.

Model I provides us with a minimal model, but it remains limited in a key aspect. It predicts slow sawtooth oscillations for the $[Ca^{2+}]_i$ that disagree with the experimental findings of Santos et al. (1991), showing that the $[Ca^{2+}]_i$ oscillations are closer to a square wave. This implies that $[Ca^{2+}]_i$ is a fast variable relative to the burst period. Furthermore, in the absence of consensus about the correct mechanism underlying bursting, it is necessary to examine whether the effects of the presence of Na^+/Ca^{2+} exchange activity are independent of the hypothesis concerning the identity of the slow variable of the system. We have thus investigated the impact of the Na^+/Ca^{2+} exchange activity on two other single-cell models where $[Ca^{2+}]_i$ is a fast variable; these models differ by the slow variable that modulates the electrical activity. Model II is a modification of a previous model (Sherman, 1996) in which the bursting activity is driven by the oscillation of a slow variable *s*, which activates a biologically unidentified hyperpolarizing current, I_{slow}. In model III bursting relies on a Ca^{2+}-activated K^+ current as in model I, but the Ca^{2+} concentration in the ER plays the role of the slow oscillating variable. In these two models, we reproduce the same qualitative effect of the Na^+/Ca^{2+} exchange current, i.e., its capability to modulate the plateau fraction.

The modulation of the plateau fraction by the Na^+/Ca^{2+} exchange activity would be of poor physiological interest in the absence of a link between the activity of the exchanger and extracellular glucose concentration. Interestingly, it has been shown that, in clusters of pancreatic β-cells, $[Na^+]_i$ is a glucose-sensitive parameter that decreases when the extracellular glucose concentration is raised. All three models show that the increased Na^+/Ca^{2+} exchange activity due to the corresponding glucose-induced $[Na^+]_i$ decrease is able to raise the plateau fraction substantially. Furthermore, it should be noted that the range of the glucose-induced $[Na^+]_i$ decrease may be greater at the submembrane level compared to the average values measured in clusters (Saha and Grapengiesser, 1995). The latter measures show a 3–4 mM $[Na^+]_i$ decrease when glucose is raised from 3 mM to 20 mM. Taking into account larger variations of submembrane Na^+ levels would allow the plateau fraction increase due to the exchange activity to be more pronounced. For example, decreasing $[Na^+]_i$ from 15 mM to 7 mM induces a plateau fraction increase of more than 20% in model III (data not shown). This shows that the exchanger could play a substantial role in the glucose-dependent regulation of the plateau fraction. However, in view of the quantitative values, it seems unlikely that it is the predominant mechanism involved in the glucose-induced increase in plateau fraction, which goes from 0 to 1.

The Na^+/Ca^{2+} exchange also seems to play an important role in the calcium regulation in clusters of gap-junctionally coupled cells. In the absence of Na^+/Ca^{2+} exchange activity, the distribution of cell parameters with a 15% standard deviation is enough to induce local $[Ca^{2+}]_i$ peaks in the

micromolar range in a few cells of the cluster. These $[Ca^{2+}]_i$ peaks are decreased when the Na^+/Ca^{2+} exchange is active. Such an effect on $[Ca^{2+}]_i$ dynamics would be impossible in the single-cell models, where the depolarizing influence of $I_{Na/Ca}$ always leads to a prolongation of the burst and an increased $[Ca^{2+}]_i$. In these models, the extrusion rate of Ca^{2+} ions from the cytosol is small compared to the amount of Ca^{2+} entering the cell through L-type Ca^{2+} channels during the burst. Therefore, the net effect of the burst prolongation is an increase of $[Ca^{2+}]_i$. In the cluster model, there is an important activation of the Na^+/Ca^{2+} exchange activity in the cells producing $[Ca^{2+}]_i$ peaks. At the level of this cell, $I_{Na/Ca}$ is much higher that in the other cells of the network, and the Na^+/Ca^{2+} exchange activity becomes a major mechanism for Ca^{2+} extrusion. In contrast to the single-cell models, the depolarizing influence of this locally elevated $I_{Na/Ca}$ is not able to prolong the burst duration excessively (i.e., allowing massive Ca^{2+} entry through the L-type Ca^{2+} channels that would more than compensate the Ca^{2+} extrusion by Na^+/Ca^{2+} exchange activity). The synchronization of the electrical activity induced by the gap-junction coupling forces the cells producing $[Ca^{2+}]_i$ peaks to repolarize at the same time as the other cells of the cluster. Therefore, the presence of the Na^+/Ca^{2+} exchange activity allows a substantial decrease in the $[Ca^{2+}]_i$ peak values. Note that this is a local effect: the average $[Ca^{2+}]_i$ in the cluster is still increased by the presence of Na^+/Ca^{2+} exchange activity as in the single cell models.

Additional numerical simulations with the multicellular model show a plateau fraction increase when $[Na^+]_i$ is decreased, which is of the same order as in the single cell models. For example, decreasing $[Na^+]_i$ from 15 mM to 9 mM induces a plateau fraction increase of 5% (results not shown).

In conclusion, we have shown that the Na^+/Ca^{2+} exchange provides a new mechanism, in addition to K-ATP channels, linking the plateau fraction with the extracellular glucose concentration. This additional mechanism available to the cell may provide more robustness to the stimulus-secretion coupling. Furthermore, our theoretical study suggests that, in addition to this regulatory role in electrical activity, the Na^+/Ca^{2+} exchange plays a crucial role in the $[Ca^{2+}]_i$ regulation of heterogeneous cells coupled by gap junctions, preventing the possible local occurrence of $[Ca^{2+}]_i$ peaks.

APPENDIX: EQUATIONS AND PARAMETER VALUES

Model I

$$C_m \frac{dV}{dt} = -I_K - I_{Ca} - I_{K(Ca)} - I_{Na/Ca}$$

$$\frac{dn}{dt} = \lambda \frac{n_\infty(V) - n}{\tau_n(V)}$$

$$\frac{dCa_i}{dt} = f[-\alpha(I_{Ca} - 2I_{Na/Ca}) - k_{Ca}Ca_i]$$

where

$$I_K = \bar{g}_k n(V - V_K)$$

$$I_{Ca} = \bar{g}_{Ca} m_\infty(V) h(V)(V - V_{Ca})$$

$$I_{K(Ca)} = \bar{g}_{K(Ca)} Ca_i/[K_d + Ca_i](V - V_K)$$

$$I_{Na/Ca} = \bar{g}_{Na/Ca} Ca_i^{n_H}/[K_{1/2}^{n_H} + Ca_i^{n_H}](V - V_{Na/Ca})$$

$$n_\infty(V) = 1/\{1 + \exp[(V_n - V)/S_n]\}$$

$$\tau_n(V) = c/\{\exp[(V - \bar{V})/a] + \exp[(\bar{V} - V)/b]\}$$

$$m_\infty(V) = 1/\{1 + \exp([V_m - V]/S_m)\}$$

$$h(V) = 1/\{1 + \exp([V_h - V]/S_h)\}$$

$$V_{Na/Ca} = RT/F[3\ln(Na_o/Na_i - \ln(Ca_o/Ca_i)]$$

Parameter values are C_m = 5310 fF, $\bar{g}_k$ = 2500 pS, $\bar{g}_{Ca}$ = 1400 pS, $\bar{g}_{K(Ca)}$ = 30,000 pS, $\bar{g}_{Na/Ca}$ = 234 pS, V_K = −75 mV, V_{Ca} = 110 mV, V_m = 4 mV, S_m = 14 mV, V_h = −10 mV, S_h = −10 mV, V_n = −15 mV, S_n = 5.6 mV, $\bar{V}$ = −75 *mV*, a = 65 mV, b = 20 mV, c = 60 ms, K_d = 100 μM, $K_{1/2}$ = 1.5 μM, n_H = 5, RT/F = 26.54 mV, $[Na^+]_o$ = 140 or 30 mM, $[Na^+]_i$ = 10 mM, $[Ca^{2+}]_o$ = 2600 μM, f = 0.001, k_{Ca} = 0.03 ms^{-1}, λ = 1.6, α = 4.5055 × 10^{-6} mol/[(μm)^{3}C].

Model II

$$C_m \frac{dV}{dt} = -I_K - I_{Ca} - I_{slow} - I_{Na/Ca}$$

$$\frac{dn}{dt} = \lambda \frac{n_\infty(V) - n}{\tau_n}$$

$$\frac{ds}{dt} = \frac{S(V, R_s) - s}{\tau_s}$$

$$\frac{d[Ca]_i}{dt} = f[-\alpha(I_{Ca} - 2I_{Na/Ca}) - k_{Ca}[Ca]_i] + k_{rel}([Ca]_{ret} - [Ca]_i) - k_{pump}[Ca]_i$$

$$\frac{d[Ca]_{ret}}{dt} = -k_{rel}([Ca]_{ret} - [Ca]_i) + k_{pump}[Ca]_i$$

with I_K, $I_{Na/Ca}$ as in model I,

$$I_{Ca} = \bar{g}_{Ca} m_\infty(V)(V - V_{Ca})$$

$$I_{slow} = \bar{g}_s s(V - V_K)$$

$$S(V, R_s) = S_\infty(V) + R_s$$

$$S_\infty = 1/\{1 + \exp([V_s - V]/S_s)\}$$

Parameters are as in Model I, except for $\bar{g}_k$ = 2700 pS, $\bar{g}_{Ca}$ = 1000 pS, $\bar{g}_s$ = 200 pS, $\bar{g}_{Na/Ca}$ = 350 pS, V_{Ca} = 25 mV, τ_n = 20 ms, τ_s = 12,000 ms, V_m = −20 mV, S_m = 12 mV, V_n = −16 mV, R_s = 0.58, V_s = −52 mV, S_s = 10 mV, f = 0.02, k_{Ca} = 0.64 ms^{-1}, λ = 1.0, α = 6 × 10^{-5} mol/[(μm)^{3}C], k_{rel} = 6 × 10^{-4} ms^{-1}, k_{pump} = 0.2 ms^{-1}.

Model III

$$C_m \frac{dV}{dt} = -I_K - I_{Ca} - I_{K(Ca)} - I_{Na/Ca}$$

$$\frac{dn}{dt} = \lambda \frac{n_\infty(V) - n}{\tau_n}$$

$$\frac{d[Ca]_i}{dt} = f[-\alpha(I_{Ca} - 2I_{Na/Ca}) - k_{Ca}[Ca]_i] + k_{rel}([Ca]_{ret} - [Ca]_i) - k_{pump}[Ca]_i$$

$$\frac{d[Ca]_{ret}}{dt} = -k_{rel}([Ca]_{ret} - [Ca]_i) + k_{pump}[Ca]_i$$

with I_K, $I_{K(Ca)}$, $I_{Na/Ca}$ as in model I and I_{Ca} as in model II. Parameters are as in Model I, except for $\bar{g}_k = 2700$ pS, $\bar{g}_{Ca} = 1000$ pS, $\bar{g}_{Na/Ca} = 1000$ pS, $V_{Ca} = 25$ mV, $K_d = 70$ μM, $k_{Ca} = 0.64$ ms^{-1}, $\lambda = 0.85$, $\alpha = 6 \times 10^{-5}$ mol/[(μm)^{3}C], $k_{rel} = 6 \times 10^{-4}$ ms^{-1}, $k_{pump} = 0.2$ ms^{-1}.

Cluster model

The parameters that have been lognormally distributed over the cellular cluster (with 15% standard deviation and mean value as in model III) are C_m, $\bar{g}_k$, $\bar{g}_{Ca}$, $\bar{g}_{K(Ca)}$, $\bar{g}_{Na/Ca}$, f, k_{rel}, k_{pump}.

The gap-junctional conductances have been distributed following an experimental histogram (Perez-Armendariz et al., 1985), as proposed by Smolen et al. (1993). Thirty percent of pairs of cells are uncoupled, and the others are coupled, with coupling conductances going from 100 to 600 pS.

The other parameters are constant and have the same value as in model III, except for $\lambda = 0.75$.

We thank Albert Goldbeter, Geneviève Dupont, and Philippe Lebrun for helpful discussions and careful reading of the manuscript and Arthur Sherman for his constructive remarks. We also thank André Herchuelz and Jean-Louis Martiel for their support.

David Gall was a grant-holder from Fonds pour la Formation à la Recherche dans l'Industrie et dans l'Agriculture (FRIA), Brussels, Belgium. Isabella Susa was supported by a grant from the European Union, TMR program (Training and Mobility of Researchers, contract ERBFM-BICT950164).

REFERENCES

Atwater, I., C. M. Dawson, B. Ribalet, and E. Rojas. 1980. The nature of oscillatory behaviour in electrical activity from pancreatic β-cell. *In* Biochemistry and Biophysics of the Pancreatic β-Cell. W. J. Malaisse and I. B. Täljedal, editors. Georg Thieme Verlag, Stuttgart. 100–107 (*Horm. Metab. Res. Suppl.* 10).

Bers, D. M. 1991. Species differences and the role of sodium-calcium exchange in cardiac muscle relaxation. *Ann. N.Y. Acad. Sci.* 639: 375–385.

Blaustein, M. P., and A. L. Hodgkin. 1969. The effect of cyanide on the efflux of calcium from squid axons. *J. Physiol. (Lond.).* 200:497–527.

Bokvist, K., L. Eliasson, C. Ämmälä, E. Renström, and P. Rorsman. 1995. Co-localisation of L-type Ca^{2+} channels and insulin-containing secretory granules and its significance for the initiation of exocytosis in mouse pancreatic B-cells. *EMBO J.* 14:50–57.

Chay, T. R. 1997. Effects of extracellular calcium on electrical bursting and intracellular and luminal calcium oscillations in insulin secreting pancreatic β-cells. *Biophys. J.* 73:1673–1688.

Dean, P. M., and E. K. Matthews. 1970. Glucose-induced electrical activity in pancreatic islet cells. *J. Physiol. (Lond.).* 210:255–264.

Egan, T. M., S. J. Noble, T. Powell, A. J. Spindler, and V. W. Twist. 1989. Sodium-calcium exchange during the action potential in guinea pig ventricular cells. *J. Physiol. (Lond.).* 41:639–661.

Ehara, T., S. Matsuoka, and A. Noma. 1989. Measurement of reversal potential of Na-Ca exchange current in single guinea-pig ventricular cells. *J. Physiol. (Lond.).* 410:227–249.

Gall, D., J. Gromada, I. Susa, A. Herchuelz, P. Rorsman, and K. Bokvist. 1999. Significance of Na/Ca exchange for Ca^{2+}-buffering and electrical activity in mouse pancreatic β-cells. *Biophys. J.* (in press).

Göpel, S., and P. Rorsman. 1998. Activation of Ca^{2+}-activated K^+-conductance terminates the burst of action potentials in insulin secreting pancreatic β cells. *Diabetologia.* 41:A540.

Hellman, B., T. Andersson, P.-O. Berggren, and P. Rorsman. 1980. Calcium and pancreatic beta-cell function. XI. Modification of ^{45}Ca fluxes by Na^+ removal. *Biochem. Med.* 24:143–152.

Herchuelz, A., A. Sener, and W. J. Malaisse. 1980. Regulation of calcium fluxes in rat pancreatic islets: calcium extrusion by sodium-calcium countertransport. *J. Membr. Biol.* 57:1–12.

Hilgemann, D. W. 1996. The cardiac Na-Ca exchanger in giant membrane patches. *Ann. N.Y. Acad. Sci.* 779:136–158.

Hilgemann, D. W., S. Matsuoka, G. A. Nagel, and A. Collins. 1992. Steady-state and dynamic properties of cardiac sodium-calcium exchange. Secondary modulation by cytoplasmic calcium and ATP. *J. Gen. Physiol.* 100:933–961.

Hodgkin, A. L., and A. F. Huxley. 1952. A quantitative description of membrane current and its application to conduction and excitation in nerve. *J. Physiol. (Lond.).* 117:500–544.

Kimura, J., A. Noma, and H. Irisawa. 1986. Na-Ca exchange current in mammalian heart cells. *Nature.* 319:596–597.

Kukuljan, M., A. Goncalves, and I. Atwater. 1991. Charybdotoxin-sensitive K-Ca channels is not involved in glucose induced electrical activity of pancreatic β-cells. *J. Membr. Biol.* 119:187–195.

Meissner, H. P. 1976. Electrophysiological evidence for coupling between β-cells of pancreatic islets. *Nature.* 262:502–504.

Meissner, H. P., and H. Schmelz. 1974. Membrane potential of beta-cells in pancreatic islets. *Pflügers Arch.* 351:195–206.

Miura, Y., and J. Kimura. 1989. Sodium-calcium exchange current. Dependence on internal Ca and Na and competitive binding of external Na and Ca. *J. Gen. Physiol.* 93:1129–1145.

Noble, D., S. J. Noble, G. C. Bett, Y. E. Earm, W. K. Ho, and I. K. So. 1991. The role of the sodium-calcium exchange during the cardiac action potential. *Ann. N.Y. Acad. Sci.* 639:334–353.

Perez-Armendariz, E., E. Rojas, and I. Atwater. 1985. Glucose-induced oscillatory changes in extracellular ionized potassium concentration in mouse islets of Langerhans. *Biophys. J.* 48:741–749.

Reuter, H., and N. Seitz. 1968. The dependence of calcium efflux from cardiac muscle on temperature and external ion composition. *J. Physiol. (Lond.).* 195:451–470.

Saha, S., and E. Grapengiesser. 1995. Glucose promotes turnover of Na^+ in pancreatic β-cells. *Biochim. Biophys. Acta.* 1265:209–212.

Santos, R., L. Rosario, A. Nadal, J. Garcia-Sancho, B. Soria, and M. Valdeomillos. 1991. Widespread synchronous Ca^{2+} oscillations due to bursting electrical activity in single pancreatic islets. *Pflügers Arch.* 418:417–422.

Sherman, A. 1996. Contributions of modeling to understanding stimulus-secretion coupling in pancreatic β-cells. *Am. J. Phys.* 271:E362–E372.

Sherman, A., J. Rinzel, and J. Keizer. 1988. Emergence of organized bursting in clusters of pancreatic β-cells by channel sharing. *Biophys. J.* 54:411–425.

Smolen, P., J. Rinzel, and A. Sherman. 1993. Why pancreatic islets burst but single β cells do not: the heterogeneity hypothesis. *Biophys. J.* 64:1668–1680.

Van Eylen, F., M. Svoboda, and A. Herchuelz. 1997. Identification, expression pattern and activity of Na/Ca exchanger isoforms in rat pancreatic β-cells. *Cell Calcium.* 21:185–193.

Wesslen, N., P. Bergsten, and B. Hellman. 1986. Glucose-induced reduction of the sodium content in β-cell-rich pancreatic islets. *Biosci. Rep.* 6:967–972.